Materials Research. 2025; 28:e20240560
DOI: https://doi.org/10.1590/1980-5373-MR-2024-0560

Effects of Etching Duration on Surface Properties and Friction/Wear Characteristics of Ceramic-Coated Silicone Rubber for Hydrogen Compressors

Sung-Jun Lee[a], Chan-Woo Kim[a], Chang-Lae Kim[a]*

[a]*Chosun University, Department of Mechanical Engineering, 61452, Gwangju, Republic of Korea.*

Received: December 07, 2024; Revised: February 17, 2025; Accepted: March 23, 2025

In this study, we explored the effects of etching on the surface properties and tribological performance of silicone rubber for hydrogen compressor applications. Ceramic particle-coated silicone rubber specimens were etched using a solution of nitric acid and ammonium fluoride for different durations. XRD and Raman analyses confirmed that the etching process did not alter the crystalline structure and molecular bonding of the PDMS matrix. EDS analysis revealed changes in surface composition after etching. The findings demonstrated that extended etching times resulted in the formation of complex surface structures, profoundly modifying the topography and wettability of silicone rubber. These surface alterations influenced the interfacial adhesion with ceramic coatings. However, prolonged etching reduced the optical transparency. Compared to bare PDMS, the ceramic-coated specimens showed enhanced wear resistance. Tribological investigations revealed an initial increase in the friction coefficient with increasing etching duration, followed by a slight decrease for the 30-minute etched specimen. Wear analysis indicated that longer etching times resulted in more severe wear tracks, implying increased surface damage and material loss.

Keywords: *Silicone rubber, Surface modification, Etching process, Friction and wear characteristics, Hydrogen compressor applications*

1. Introduction

Hydrogen has emerged as a promising clean energy source because of its high energy density and low carbon emissions during combustion[1,2]. Efficient and reliable hydrogen storage and transportation systems are essential to facilitate the widespread application of hydrogen energy[3]. Hydrogen compressors play a crucial role in storing and transporting high-pressure compressed gases, and their performance and lifespan are determined by the mechanical strength and corrosion resistance of their components[4,5]. These components are exposed to harsh operating conditions such as high pressure, high temperature, and corrosive environments, which can lead to premature failure and reduced compressor efficiency. Silicone rubber, a commonly used material for sealing compressors, is known for its excellent corrosion resistance, thermal stability, and elasticity[6-9]. Although it has high gas permeability compared to other elastomers, silicone rubber has excellent heat resistance, chemical resistance, and elasticity, making it suitable for the harsh operating conditions of hydrogen compressors[10]. Silicone rubber can maintain stable properties over a wide temperature range and exhibits good resistance to acidic and basic environments[7]. In addition, silicone rubber's low Young's modulus and high elasticity help improve the sealing performance and reduce friction between the compressor parts[11].

These properties make silicone rubber an ideal material for maintaining compressor seals, preventing leakage, and ensuring an efficient operation. However, silicone rubber is prone to wear when in contact with other components such as pistons and cylinders, which can result in leakage and performance degradation[12].

To address these issues, various surface modification techniques have been investigated to improve the durability and friction performance of silicone rubber without compromising its corrosion resistance[13-15]. Surface texturing and coating have been explored as potential methods to enhance the surface properties of silicone rubber. Among these approaches, coating with ceramic materials has proven effective in improving the mechanical strength and wear resistance of silicone rubber[16,17]. Incorporating ceramic particles onto the silicone rubber surface can not only enhance the mechanical properties by forming a coating layer but also act as a mask during the etching process, creating specific surface roughness and texture. Furthermore, the presence of coating particles on the surface can modify the contact mechanics and stress distribution at the interface, thereby reducing local stresses that can cause material wear[18].

However, the influence of optimal coating conditions and subsequent surface treatments on the friction and wear behaviors of silicone rubber has not been investigated from the perspective of hydrogen compressor applications.

The surface modification through ceramic particle coating and etching applied in this study has the potential to improve the gas barrier properties of silicone rubber. The micro/nanostructures formed on the surface can complicate the diffusion paths of gas molecules and reduce the gas permeability[19]. In addition, the oxidation of silicone rubber during the etching process

*e-mail: kimcl@chosun.ac.kr

can result in the formation of polar groups on the surface, which reduces the gas solubility[20]. Therefore, if the gas barrier properties of silicone rubber can be improved through surface modification, its suitability as a seal material for hydrogen compressors can be further enhanced.

Among the various subsequent surface treatment processes, etching has been employed to create micro/nanoscale surface structures on various materials, including polymers and ceramics, to improve the surface properties and friction performance. The formation of these surface microstructures can increase the surface roughness and create additional hierarchical structures in the coating layer, thereby reducing direct contact between the sliding surfaces and mitigating wear.

Previous studies have demonstrated the effectiveness of surface texturing through etching in enhancing the frictional properties of various materials. Mei et al. proposed a method for creating surface structures on molds via chemical etching[21]. They etched the surface of the Cr12 samples to form various surface structures and investigated their surface morphology and wear resistance. The study found that etched surfaces could effectively reduce the friction coefficient of molds under high-load conditions, with a maximum friction coefficient reduction rate of 49.5%. Mirmohammadi et al. conducted a study on the fabrication and characterization of PDMS/Cu composites[22]. The PDMS/Cu composites were fabricated by replicating the microstructures of the etched aluminum substrates. To confirm the durability of the fabricated composites, stretching, wear, and bending tests were performed, and the wear resistance due to changes in the surface structure was analyzed through friction tests. The study found that the wear resistance of the surface changed when the number of friction cycles exceeded 1,500, with a notable decrease in the wear resistance observed at friction cycles above 3,000.

Although these studies demonstrate the potential of surface modification techniques, the specific effects of etching parameters, such as etching time, on the surface properties and tribological performance of ceramic-coated silicone rubber remain to be explored in detail. Understanding these relationships is crucial for guiding the optimization of etching processes for silicone rubber components in demanding applications, such as hydrogen compressors.

This study aimed to investigate the influence of etching time on the surface characteristics and tribological behavior of ceramic-coated silicone rubber. By systematically varying the etching duration and characterizing the resulting surface morphology, roughness, wettability, and friction/wear properties, we sought to elucidate the underlying mechanisms and potential optimization strategies for silicone rubber components in hydrogen compressors. Through achieving these objectives, the results of this study will provide valuable fundamental data for the design and development of surface engineering technologies for silicone rubber components in hydrogen compressors and related applications. Optimizing surface modification conditions can lead to the design of silicone rubber surfaces with improved durability, enhanced friction/wear characteristics, and maintained corrosion resistance, ultimately contributing to more efficient and sustainable hydrogen storage and transportation systems.

2. Experimental Details

2.1. Materials

In this study, a combined fabrication approach involving a ceramic coating and etching was employed to produce silicone rubber with various surface structures. Figure 1 illustrates a schematic of the specimen fabrication process used to create different surface structures on silicone rubber. The silicone rubber base and curing agent (Sylgard 184, DOW Hitech, Goyang, Republic of Korea) were mixed at a weight ratio of 10:1, and a heat-curing method was used. First, after mixing the silicone rubber base and curing agent, the mixture was heated at 70 °C for 10 min, and ceramic particles (iM30K, 3M, Seoul, Republic of Korea) were coated on the surface of the silicone rubber. Subsequently, the specimens were heated to 70 °C for approximately 2 h to achieve a complete curing. The ceramic particles coated on the silicone rubber surface are spherical ceramic particles with diameters of 10-30 μm, which have high mechanical strength and wear resistance.

An etching process was employed to form micro-/nanostructures on the surface of the silicone rubber. The etching solution was prepared by mixing 35 wt% nitric acid (HNO_3, Sanchun Chemicals Co. Ltd., Pyeongtaek, Republic of Korea) and ammonium fluoride (NH_4HF_2, Sanchun Chemicals Co. Ltd., Pyeongtaek, Republic of Korea) in a 2:1 weight ratio. The ceramic particle-coated silicone rubber was etched in the etching solution for 1, 5, 10, and 30 min, immersed in deionized water, and subjected to ultrasonic

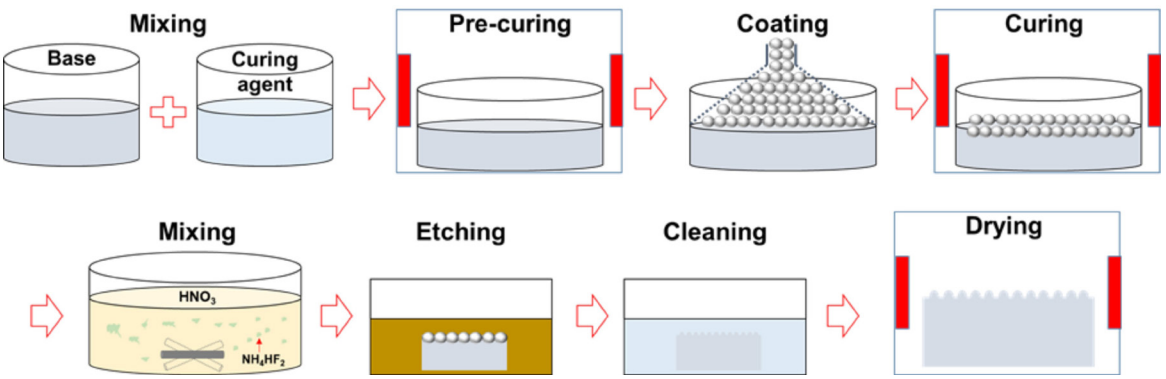

Figure 1. Schematic of specimen fabrication process using ceramic coating and etching.

treatment for 15 min. The specimens were then dried in a convection oven for approximately 1 h.

2.2. Experiments

Low-voltage scanning electron microscopy (LV-SEM; JSM-IT300, Jeol, Tokyo, Japan) was employed to analyze the surface morphology of the silicone rubber specimens according to the etching time. The chemical composition of the etched surfaces was investigated using energy-dispersive X-ray spectroscopy (EDS) coupled with the LV-SEM.

X-ray diffraction (XRD; Empyrean, Panalytical, Malvern, UK) analysis was conducted to identify the crystalline phases present in the ceramic coating layer and to assess the changes in the crystal structure induced by the etching process. The XRD patterns were recorded using Cu Kα radiation (λ = 1.5406 Å) in the 2θ range of 5-30° with a step size of 0.01°.

Raman spectroscopy (Dimension Edege, Bruker, Texas, USA) was performed to characterize the molecular structure and bonding states of the silicone rubber and ceramic coating.

The surface wettability of silicone rubber was evaluated using contact angle measurements. A 10 μL droplet of deionized water was placed on the specimen surface, and the angle formed by the water droplet was measured. The contact angle was averaged from the measurements obtained at five or more locations on each specimen.

To assess the effect of the etching time on the surface morphology of the silicone rubber, the surface roughness was measured using a 2D profilometer (SV-2100M4, Mitutoyo Co., Ltd., Kawasaki-shi, Japan). A stylus with a tip radius of 2 μm was used to scan a length of 2 mm on the specimen surface at a speed of 0.5 mm/s and a load of 0.75 mN. The average surface roughness (Ra) was calculated from three measurements obtained from different locations on each specimen.

The optical properties of the silicone rubber specimens were investigated using a UV-visible spectrophotometer (Libra S22, Biochrom Ltd., Cambridge, UK) in the wavelength range–300-900 nm. To evaluate the effect of the etching time on the optical transparency of the silicone rubber, the transmission spectra of the specimens were recorded.

The friction and wear characteristics of silicone rubber were evaluated using a reciprocating sliding-type friction tester (RFW 160, NEOPLUS Co., Ltd, Daejeon, Republic of Korea). A 220-grit sandpaper with a diameter of 2 mm was used as the countertip to simulate the rough surfaces of the piston and cylinder in a hydrogen compressor. The rough surface of the sandpaper was selected to represent the worst-case scenario, where the piston or cylinder surface might have been damaged or worn, leading to increased surface roughness and abrasive wear. The tests were conducted under a vertical load of 20 mN, a sliding distance of 2 mm, and a sliding speed of 4 mm/s for 2,000 cycles. The friction coefficient was continuously recorded during the test and the average friction coefficient for each specimen was calculated. After the friction test, the wear morphology of the silicone rubber was analyzed using a scanning electron microscope.

All experimental measurements (contact angle, surface roughness, optical properties, and friction/wear tests) were repeated at least three times under identical conditions, and the average values were used for analysis.

3. Results and Discussion

The chemical effects of the etching process on the silicone rubber surface can be inferred from the composition of the etching solution, which contains nitric acid (HNO_3) and ammonium fluoride (NH_4HF_2). During the etching process, nitric acid may oxidize the silicone rubber, leading to the formation of polar functional groups, such as silanol (Si-OH), on the surface[23]. These polar groups can contribute to the observed changes in the wettability by increasing the surface energy of the etched specimens. Additionally, the ammonium fluoride in the etching solution may react with the silicone rubber, leading to the formation of soluble silicon fluoride compounds and subsequent dissolution of the silicone matrix. This selective dissolution process can result in the formation of micro- and nanoscale surface features. The combined effects of surface oxidation and dissolution during the etching process can significantly alter the surface chemistry and morphology of silicone rubber, ultimately influencing its wettability and tribological behavior.

As shown in Figure 2, the LV-SEM images reveal the evolution of the surface morphology of the silicone rubber as a function of the etching time. The bare PDMS specimen exhibited a remarkably smooth surface morphology, with no discernible surface features or irregularities. This observation is consistent with the inherent characteristics of PDMS, which is known for its excellent surface smoothness and low surface roughness. The absence of any surface structures on the bare PDMS serves as a reference point for evaluating the effects of the ceramic coating and subsequent etching process on the surface morphology of the silicone rubber specimens.

The unetched silicone rubber specimen appeared to have a relatively rough surface, with only ceramic particles observed on the silicone rubber surface. This indicated that the ceramic particles coated on the silicone rubber surface significantly altered the overall topography. The surface of the specimen etched for 1 min exhibited microstructure development. Small pits and grooves were observed, suggesting that the etching process began to selectively remove silicone material around the ceramic particles. The specimen etched for 5 min exhibited a more pronounced surface texture, with the formation of a network of interconnected microscale structures. As etching progressed, more complex and irregular surface morphologies were formed. After 10 min of etching, the surface structure became much more intricate with the development of both the micro/nanoscale features. The images reveal a highly porous and hierarchical surface topography, indicating that the silicone rubber was substantially removed by etching, resulting in a considerably rough surface. For the specimen etched for 30 min, the surface structure became even more complex with the development of the micro/nanoscale features. The images show a highly porous and hierarchical surface topography, suggesting that the silicone rubber was extensively removed by etching, leading to an extremely rough surface. The specimen etched for 30 min exhibited a significant increase in the complexity of its surface structure. The surface is covered with a dense array of micro/nanosized features, creating an extremely irregular and textured morphology[24]. Extensive etching resulted in the formation of a highly porous and irregular surface.

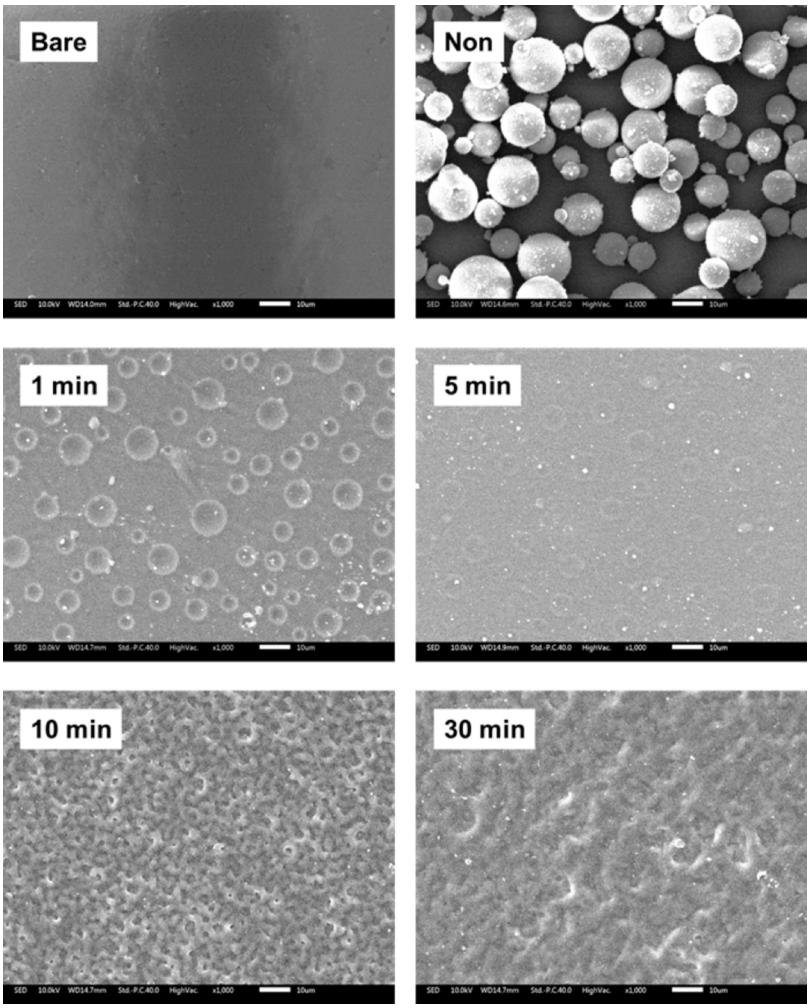

Figure 2. SEM images of silicone rubber specimens according to etching time.

Overall, the SEM images demonstrate the gradual evolution of the surface structure as a function of etching time. The surface progressively transformed into a complex and hierarchical topography with the formation of micro/nanoscale features. This evolution is a direct result of the selective removal of the silicone material during the etching process, which is facilitated by ceramic particle coating. The degree of surface structuring can be controlled by adjusting the etching time, enabling the fabrication of silicone rubber with a wide range of surface morphologies.

Figure 3 presents the EDS analysis results, revealing the elemental composition of the silicone rubber specimens at different stages of the fabrication process. The bare PDMS specimen exhibited a composition of 48.89 wt% carbon, 25.9 wt% oxygen, and 25.21 wt% silicon, which is consistent with the typical composition of PDMS. However, the ceramic particle-coated specimen (Non) showed an increase in the silicon content, reaching 44.98 wt%, accompanied by a slight decrease in the carbon content. This increase in silicon content can be attributed to the presence of the ceramic particles, which are primarily composed of silicon-based compounds.

The etched specimens demonstrated a different trend in their elemental composition. Although the silicon content in the etched specimens remained higher than that of the bare PDMS, it decreased to approximately 37 wt% compared to the non-etched specimen. This decrease in silicon content after etching might be due to the partial removal of the ceramic particles during the etching process or the exposure of the underlying PDMS matrix.

The EDS analysis did not detect the presence of fluorine or nitrogen in the etched specimens. This finding suggests that the etching process and subsequent cleaning steps did not introduce any impurities into the composite material. The absence of these elements indicates the stability and purity of the fabricated silicone rubber composites, even after undergoing the etching treatment.

Figure 4 presents the XRD patterns of the Bare, Non, 1 min, and 30 min silicone rubber specimens. All specimens exhibited a distinct peak at approximately 11°, which can be attributed to the crystalline structure of the PDMS matrix. The presence of this peak in all specimens, regardless of the surface modification process, suggests that the underlying PDMS structure remains largely unaffected by the ceramic coating and etching treatments.

The similarity in the XRD patterns among the specimens indicates that the ceramic coating and etching processes do

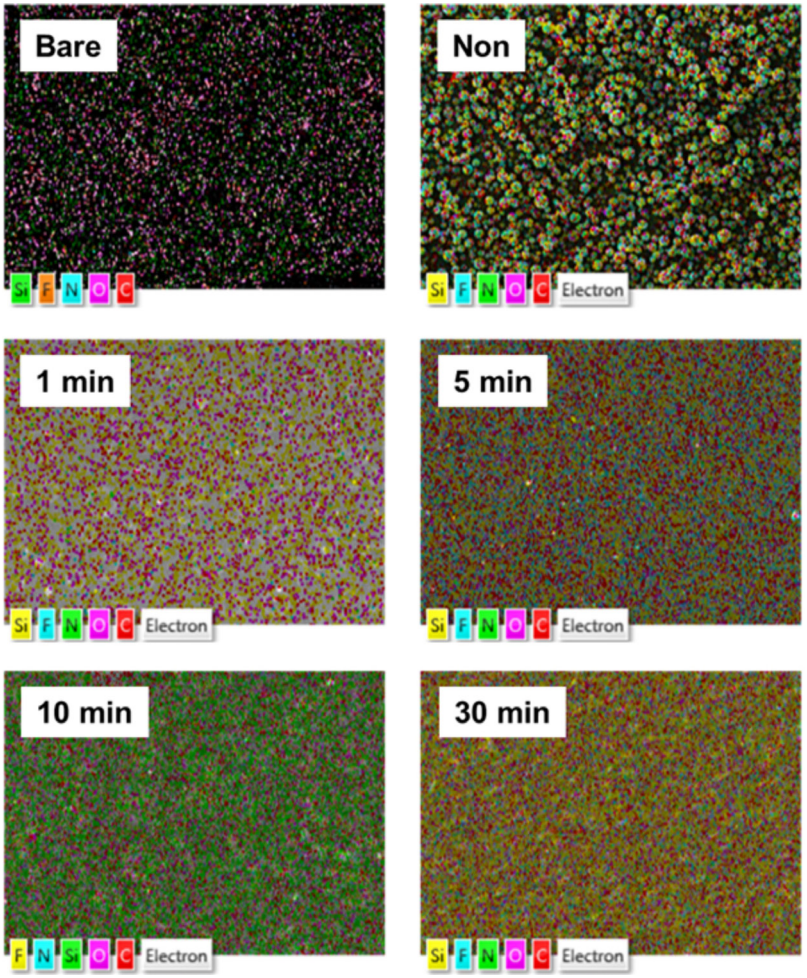

Figure 3. EDS analysis results of silicone rubber specimens with different surface conditions.

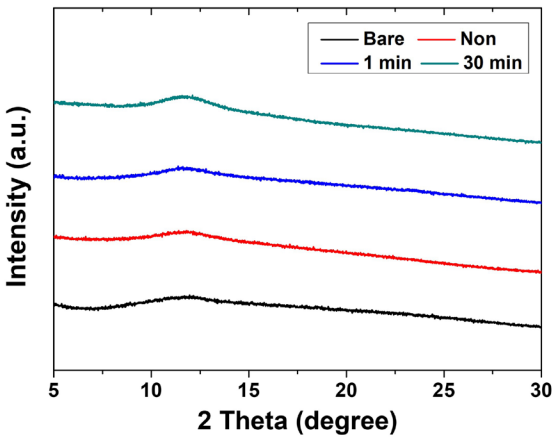

Figure 4. XRD patterns of silicone rubber specimens with different etching times.

not induce significant changes in the crystalline structure of the silicone rubber. The absence of additional peaks or shifts in the peak positions further supports the idea that the surface modifications primarily affect the surface morphology and composition of the specimens without altering the bulk crystalline structure.

These XRD results are consistent with the expected behavior of silicone rubber composites, where the PDMS matrix maintains its inherent crystalline structure while the surface modifications, such as ceramic particle coating and etching, primarily influence the surface properties and topography. The stability of the crystalline structure across different specimens highlights the compatibility and structural integrity of the fabricated silicone rubber composites.

Figure 5 displays the Raman spectra of the Bare, Non, 1 min, and 30 min silicone rubber specimens. All specimens exhibited characteristic peaks at 613, 706, 1,258, 1,409, 2,903, and 2,963 cm^{-1}, which can be assigned to the vibrational modes of the PDMS matrix[25]. The presence of these peaks in all specimens confirms that the molecular structure of the PDMS remains largely unaffected by the ceramic coating and etching processes.

However, the Non specimen showed a notable decrease in the overall intensity of the Raman peaks compared to the other specimens. This decrease in intensity can be attributed to the presence of the ceramic particles on the surface, which may attenuate the Raman signal of the underlying PDMS matrix. The ceramic particles can scatter or absorb the incident laser light, reducing the amount of light that reaches the PDMS and subsequently decreasing the intensity of the Raman peaks.

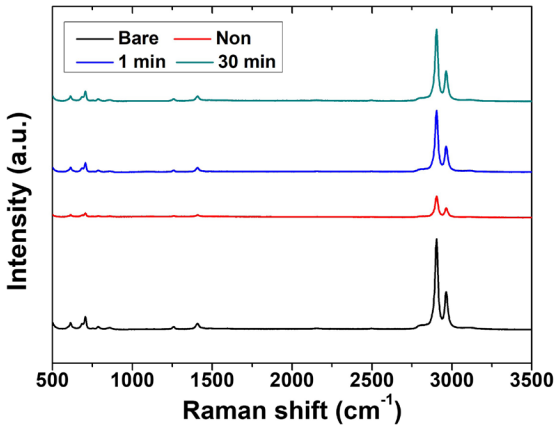

Figure 5. Raman spectra of silicone rubber specimens with different etching times.

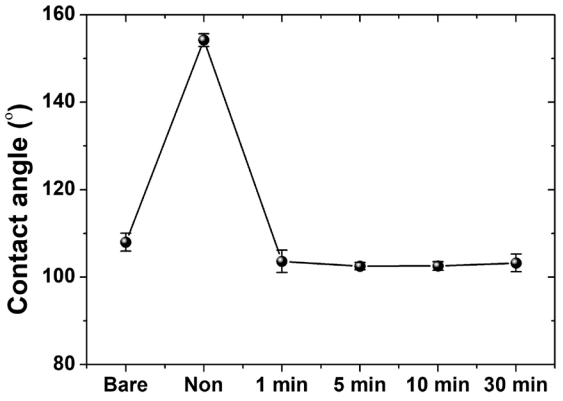

Figure 6. Contact angles of silicone rubber specimens with different etching times.

The similarity in the peak positions among the specimens suggests that the ceramic coating and etching processes do not induce significant changes in the molecular structure or bonding states of the PDMS. The consistent peak positions indicate that the surface modifications do not alter the fundamental vibrational modes of the silicone rubber.

These Raman results complement the XRD findings, confirming that the surface modifications primarily affect the surface properties and morphology of the silicone rubber specimens without significantly altering the bulk molecular structure. The decreased intensity observed in the Non specimen highlights the influence of the ceramic particles on the Raman signal, while the overall similarity in peak positions demonstrates the stability and compatibility of the fabricated silicone rubber composites.

As shown in Figure 6, the wettability of the silicone rubber specimens was evaluated by contact angle measurements. The bare PDMS specimen exhibited a water contact angle of 105.75°, which is consistent with the intrinsic hydrophobic nature of PDMS. This hydrophobicity arises from the low surface energy of PDMS due to its methyl groups (CH_3) present on the surface. In contrast, the non-etched specimen exhibited a higher water contact angle of 154°, indicating a superhydrophobic surface. This superhydrophobicity can be attributed to the hierarchical roughness introduced by the ceramic particles on the silicone rubber surface, which can trap air pockets and reduce the contact area between the water droplet and surface[26]. However, the etched specimens exhibited a significant decrease in the contact angle, with values ranging from 103° to 104°. This reduction in contact angle suggests a transition from a superhydrophobic to a less hydrophobic state, closer to the intrinsic wettability of smooth PDMS (contact angle ≈ 109°)[27,28].

The observed changes in wettability can be explained by considering the interplay between the surface roughness and surface chemistry. The initial superhydrophobicity of the non-etched specimen is a result of the hierarchical roughness created by the ceramic particles, which can promote a Cassie-Baxter wetting state, where air pockets are trapped beneath the water droplet[29]. In the initial stages of etching, the ceramic particles acted as a mask, inducing non-uniform etching. As etching progressed, the particles were gradually removed, resulting in the formation of micro-scale roughness and texture on the silicone rubber matrix. These surface morphology changes promoted the transition to a Wenzel state[30]. Additionally, the etching process may alter the surface chemistry of silicone rubber by introducing polar functional groups (e.g., hydroxyl and carboxyl), further contributing to the reduction in hydrophobicity[31].

It is important to note that the relationship between surface roughness and wettability is complex and depends on factors such as surface chemistry, surface morphology, and specific wetting regime (Cassie-Baxter or Wenzel)[32]. In this study, the observed decrease in the contact angle after etching can be attributed to the combined effects of the reduced surface roughness, removal of hydrophobic ceramic particles, and potential changes in surface chemistry.

As shown in Figure 7, the surface roughness analysis revealed that the bare PDMS specimen exhibited a relatively low surface roughness, with an average surface roughness (Ra) of 0.078 μm. In contrast, the surface roughness analysis revealed that the surface roughness of the non-etched specimen was relatively high, owing to the presence of ceramic particles on the silicone rubber surface. The average surface roughness (Ra) was 1.49 μm for the non-etched specimen, while it ranged from 0.08 μm to 0.24 μm for the etched specimens. After short etching times (1 and 5 min), the surface roughness decreased significantly, suggesting the partial removal of the ceramic particles. This decrease in roughness can be attributed to the etching solution selectively attacking the silicone rubber matrix around the ceramic particles, leading to detachment from the surface. However, as the etching time was increased to 10 and 30 min, the surface roughness increased again, surpassing that of the short-etched specimen. This increase in roughness at longer etching times can be ascribed to the formation of more complex surface morphologies with the development of micro- and nanoscale features on the silicone rubber surface[33]. Prolonged exposure to the etching solution removed the ceramic particles and selectively etched the silicone rubber matrix, creating a highly textured and hierarchical surface structure. The size, shape, and distribution of these surface features vary depending on the etching conditions such as the composition of the etching solution, etching time, and temperature.

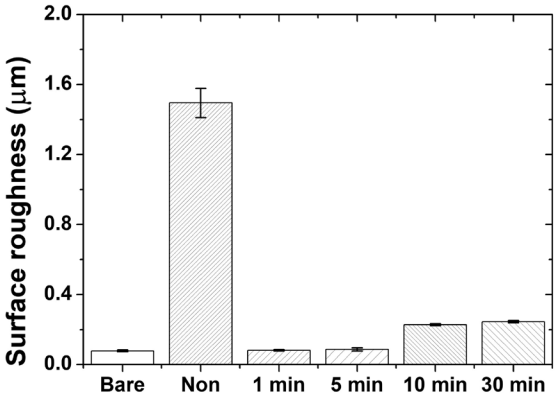

Figure 7. Surface roughness of silicone rubber specimens as a function of etching time.

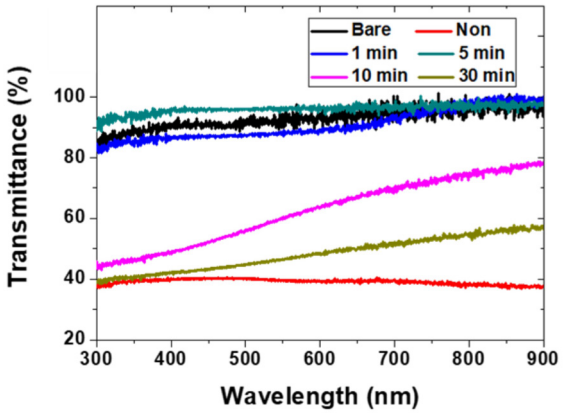

Figure 8. UV-VIS transmittance spectra of silicone rubber specimens etched for different times.

The evolution of surface roughness with etching time can be further understood by considering the role of the ceramic particles in the coating layer. The initial high surface roughness of the non-etched specimen was primarily due to the presence of these hard, micrometer-sized particles protruding from the silicone rubber surface. As the etching process began, the acidic solution preferentially attacked the silicone rubber matrix surrounding the ceramic particles, leading to their gradual detachment and a subsequent decrease in surface roughness. However, as the etching time increased, the exposed silicone rubber surface underwent further erosion and texturing, resulting in the formation of intricate micro- and nanoscale features that contributed to the increased surface roughness observed for longer etching durations.

As shown in Figure 8, the UV-VIS spectroscopy results revealed that the transmittance values of the bare PDMS specimen were similar to those of the 1 min and 5 min etched specimens, particularly in the visible-light region. The high transmittance of the bare PDMS can be attributed to its inherent optical clarity and transparency, which is a well-known characteristic of PDMS materials.

However, the non-etched specimen exhibited lower transmittance values compared to the bare PDMS and etched specimens. This reduction in transmittance can be ascribed to the presence of ceramic particles on the surface, which can scatter and absorb incident light, thereby reducing the overall optical transparency of the specimen.

The transmittance values of the etched specimens initially increased compared to the non-etched specimen, approaching the values of the bare PDMS for the 1 min and 5 min etched specimens. This increase in transmittance suggests that the etching process effectively removes the ceramic particles from the surface, reducing the scattering and absorption of light and enhancing the optical transparency.

However, as the etching time increased to 10 and 30 min, the transmittance values gradually decreased, indicating a reduction in optical transparency. This decrease in transmittance can be attributed to the formation of micro/nanoscale structures on the etched surface, which can scatter and absorb incident light[34]. The surface features generated by prolonged etching can trap light, increasing the optical path length and promoting absorption, leading to a decrease in the overall transmittance.

Figure 9 shows the evolution of the friction coefficient of the silicone rubber specimens with different etching times, including the bare PDMS, over 2,000 cycles. The bare PDMS specimen exhibited a high initial friction coefficient of over 1.8 and maintained this high friction force throughout the test without significant changes. The high friction coefficient of bare PDMS can be attributed to its inherent surface properties, such as its relatively smooth surface and high adhesion to the counter surface.

In contrast, the non-etched specimen exhibited an initial friction coefficient of 0.7, which gradually increased as the sliding cycles progressed, ultimately reaching a value of 1.25 at the end of the test. The steady increase in the friction coefficient can be attributed to the progressive wear and surface deformation of the non-etched silicone rubber, resulting in increased contact area and adhesive friction. The specimen etched for 1 min started with a relatively high initial friction coefficient of 1.4 and displayed a distinct frictional behavior. However, the friction coefficient gradually decreased until 200 cycles and then remained stable with minimal fluctuations. The initial reduction in friction can be attributed to the running-in period, where surface asperities are smoothed, and conformity between the mating surfaces is achieved. The specimen etched for 5 min commenced with an initial friction coefficient of 1.36 and exhibited a consistent increase throughout the sliding cycles, reaching a final value of 1.4. This gradual increase in friction occurred because of the progressive wear and surface damage of the etched silicone rubber, resulting in increased surface roughness and abrasive friction. The initial friction coefficient for the specimen etched for 10 min was 1.3, which increased continuously as the number of sliding cycles progressed. At the end of 2,000 cycles, the friction coefficient reached 1.55. This substantial increase in friction can be attributed to the increased contact pressure and plowing friction caused by the extensive surface damage and material removal due to the prolonged etching process. The specimen etched for 30 min started with a relatively low initial friction coefficient of 0.8 and exhibited a unique frictional behavior. However, during the first 30 cycles, the friction coefficient rapidly increased to approximately 1.3. Subsequently, it showed a gradually increasing trend, eventually reaching a value of 1.45 at the

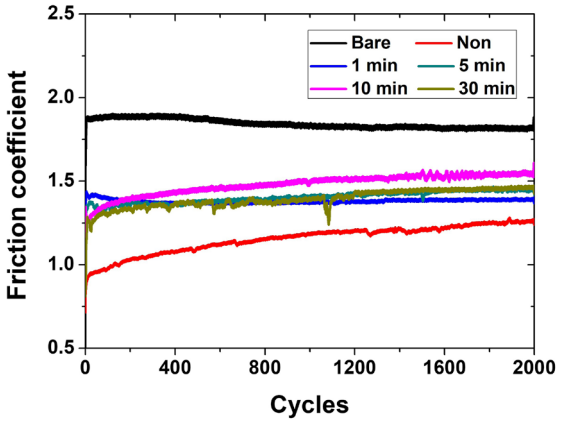

Figure 9. Friction coefficients of silicone rubber specimens with different etching times over 2,000 cycles.

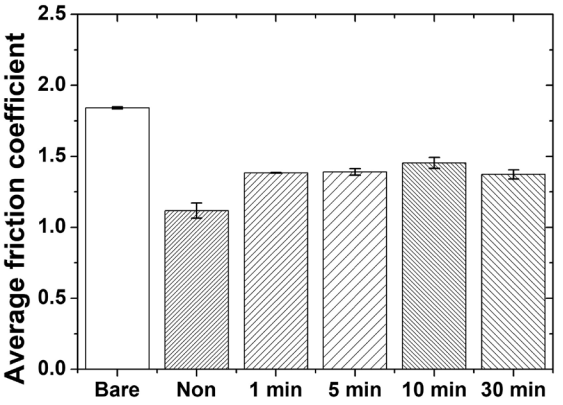

Figure 10. Average friction coefficient of silicone rubber specimens according to etching time.

end of the test. This rapid initial increase in friction can be attributed to the extensive surface roughness and presence of micropores caused by the prolonged etching process, which can lead to an increased contact pressure between the mating surfaces and physical interlocking.

Figure 10 shows the average friction coefficient values of silicone rubber specimens with different etching times. The bare PDMS specimen exhibited the highest average friction coefficient of 1.84 among all the specimens tested. This high friction coefficient can be attributed to the inherent surface properties and low mechanical properties of PDMS. In comparison, the non-etched specimen exhibited the lowest average friction coefficient of 1.12. As the etching time increased, the average friction coefficient initially increased and then slightly decreased. The specimens etched for 1, 5, and 10 min exhibited higher average friction coefficients of 1.38, 1.39, and 1.45, respectively, than the unetched specimen. However, the specimen etched for 30 min exhibited a slight decrease in the average friction coefficient to 1.37. The initial increase in the friction coefficient with increasing etching time can be attributed to the changes in the surface morphology and roughness. As the etching process progressed, the ceramic particles were partially removed, creating micron-sized pores and increasing surface roughness. This increased roughness can lead to higher contact pressures and plowing friction, resulting in higher friction coefficients for the etched specimens than for the non-etched specimen. The slight decrease in the friction coefficient of the specimen etched for 30 min can be explained by the extensive removal of the ceramic particles and the formation of a porous surface. The presence of numerous micron-sized pores can reduce the direct contact between the mating surfaces, leading to a slightly lower friction coefficient[35].

Figure 11 shows the SEM images of the wear tracks on the silicone rubber specimens after the friction test. The bare PDMS specimen exhibited the most severe wear among all the tested specimens, with rough wear tracks observed throughout the entire surface. This poor wear resistance can be attributed to the low mechanical strength and high friction force of bare PDMS, as well as the rough surface of the counter material. During the fatigue process, the wear tracks on the bare PDMS surface were formed by tearing and delamination, leading to the rapid progression of wear. In contrast, the non-etched specimen and the specimen etched for 1 min exhibited relatively smooth wear tracks with minimal surface damage, indicating excellent wear resistance. As the etching time increased, the wear tracks became more pronounced, with increased surface deformation and material removal. The specimen etched for 5 min exhibited wear morphologies with noticeable surface irregularities and some material removal. The specimen etched for 10 min exhibited a more severe wear track, with increased surface deformation and wider regions of material removal. The specimen etched for 30 min exhibited the most pronounced wear track, characterized by extensive surface damage, deep grooves, and substantial material loss. The progression of wear with increasing etching time can be attributed to the changes in the surface morphology and the presence of micron-sized pores. As the etching process removes ceramic particles and creates a porous surface, silicone rubber becomes more susceptible to wear[36]. Micron-sized pores can act as stress concentrators, leading to increased surface deformation and material removal during friction tests.

Figure 12 illustrates the proposed wear mechanisms for the non-etched and etched silicone rubber specimens during the friction test. The proposed wear mechanisms highlight the complex interplay between surface morphology, contact mechanics, and material properties in determining the tribological behavior of silicone rubber. For the non-etched specimen (Figure 12a), the wear mechanism was primarily governed by the presence of the hard ceramic particles on the surface. These particles can act as abrasive agents, leading to microcutting and microplowing of the softer silicone rubber matrix. As the sliding progresses, the ceramic particles may detach from the surface and contribute to three-body abrasive wear, further increasing the wear rate of the silicone rubber.

In contrast, the wear mechanism of the etched specimens (Figure 12b) was influenced by the surface morphology and the presence of micro- and nanoscale features generated during the etching process. The etched surface exhibited an increased density of micropores and asperities, which can alter the contact mechanics and stress distribution at the interface. These surface features can act as stress concentration sites, promoting localized plastic deformation

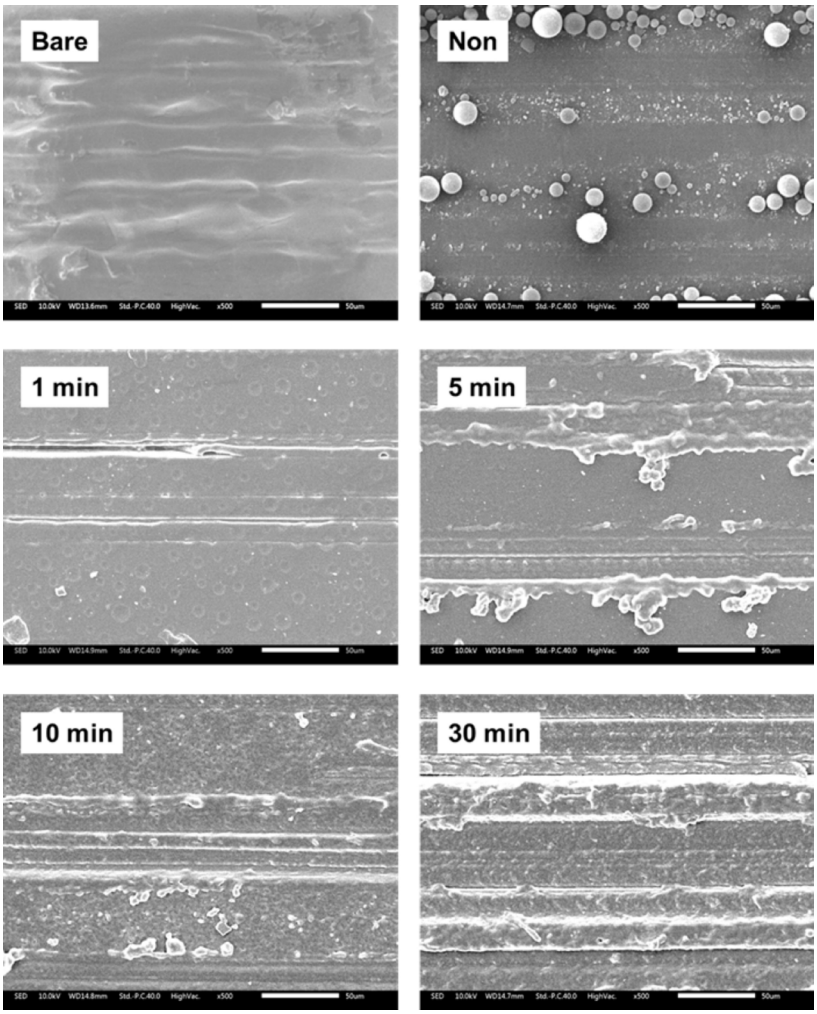

Figure 11. SEM images of wear tracks on silicone rubber specimens after friction testing.

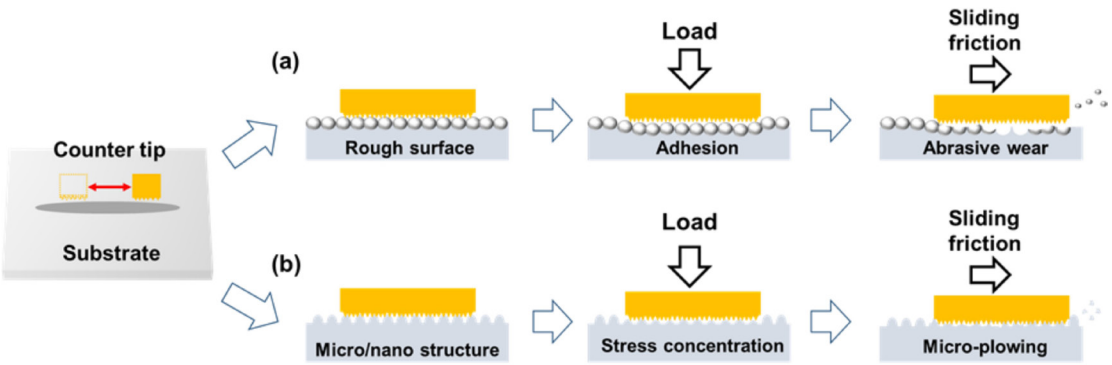

Figure 12. Schematic illustration of wear mechanisms for (a) non-etched and (b) etched silicone rubber specimens.

and material removal[37]. As the sliding progresses, the micro- and nanoscale features may be gradually worn down, leading to the exposure of the underlying silicone rubber matrix. Detached wear debris, which may consist of both silicone rubber and oxidized particles (e.g., silica), can contribute to three-body abrasive wear, leading to increased surface damage and material loss.

4. Conclusion

This study revealed the significant influence of etching time on the surface properties and tribological performance of ceramic-coated silicone rubber. The etching process induces substantial changes in the surface morphology, creating hierarchical structures that modify the topographical features

and wetting properties of the silicone rubber. XRD and Raman analyses demonstrated that the bulk crystalline structure and molecular bonding remained unchanged after surface modification. Surface composition changes were confirmed through EDS analysis. These surface modifications affect the interfacial interactions and tribological performance of the material.

The wear mechanism analysis revealed the underlying tribological phenomena, highlighting the interplay between surface morphology, contact mechanics, and material properties. The bare PDMS exhibited poor wear resistance with severe surface damage, while the non-etched specimens primarily exhibited adhesive and abrasive wear. The etched specimens demonstrated a more complex wear behavior governed by the micro/nanoscale surface features. The surface irregularities and pores induced by etching act as initiation sites for localized plastic deformation and material removal. Detached wear particles can become trapped within pores, resulting in a three-body abrasive wear mechanism.

To enhance the practicality and reliability of these findings, future studies should focus on investigating the effects of various etching parameters and conducting long-term durability assessments under realistic operating conditions. Further advancements and in-depth investigations into this surface modification technique can contribute to the development of durable silicone rubber components for hydrogen compressors and other applications.

5. Acknowledgments

This work was supported by the National Research Foundation of Korea(NRF) grant funded by the Korea government(MSIT) (No. RS-2023-00219369, RS-2024-00349019).

6. References

1. Xu X, Zhou Q, Yu D. The future of hydrogen energy: bio-hydrogen production technology. Int J Hydrogen Energy. 2022;47(79):33677-98.
2. Sezgin B, Devrim Y, Ozturk T, Eroglu I. Hydrogen energy systems for underwater applications. Int J Hydrogen Energy. 2022;47(45):19780-96.
3. Wang L, Jiao S, Xie Y, Xia S, Zhang D, Zhang Y, et al. Two-way dynamic pricing mechanism of hydrogen filling stations in electric-hydrogen coupling system enhanced by blockchain. Energy. 2022;239:122194.
4. Lee S-J, Kim C-L. Evaluation of friction and wear characteristics of carbon-based solid lubricant films for surface application of compressor parts. Tribol Lubr. 2022;38(5):222-6.
5. Lee S-J, Kim C-L. Evaluation of scratch characteristics of diaphragm for application of hydrogen compressor parts. Tribol Lubr. 2023;39(5):212-5.
6. Lee S-J, Kim C-L. Influence of surface structure on friction and wear characteristics of silicone rubber for hydraulic rod seals. RSC Advances. 2023;13(48):33595-602.
7. Zhang Z, Zhang Z, Yue S, Jiang X, Hu J. Performance characteristics of silicone rubber for use in acidic environments. Polymers (Basel). 2023;15(17):3598.
8. Zheng Y, Tan Y, Zhou C, Chen G, Li J, Liu Y, et al. A review on effect of hydrogen on rubber seals used in the high-pressure hydrogen infrastructure. Int J Hydrogen Energy. 2020;45(43):23721-38.
9. Kang HM, Choi MC, Lee JH, Yun YM, Jang JS, Chung NK, et al. Effect of the high-pressure hydrogen gas exposure in the silica-filled EPDM sealing composites with different silica content. Polymers (Basel). 2022;14(6):1151.
10. Hu W-J, Xia QQ, Pan HT, Chen HY, Qu YX, Chen ZY, et al. Green and rapid preparation of fluorosilicone rubber foam materials with tunable chemical resistance for efficient oil–water separation. Polymers (Basel). 2022;14(8):1628.
11. Feng L, Li S, Feng S. Preparation and characterization of silicone rubber with high modulus via tension spring-type crosslinking. RSC Advances. 2017;7(22):13130-7.
12. Johnson CL, Dunn AC. Wear mode control of polydimethylsiloxane (PDMS) by load and composition. Wear. 2019;438:203066.
13. Ryu B-H, Kim D-E. Development of highly durable and low friction micro-structured PDMS coating based on bio-inspired surface design. CIRP Ann. 2015;64(1):519-22.
14. Wang D-Y, Kim C-L, Kim D-E. Development of flexible polymer sheet with high surface durability using discretely embedded micro-balls. CIRP Ann. 2017;66(1):527-30.
15. Kim S, Hwang HJ, Cho H, Choi D, Hwang W. Repeatable replication method with liquid infiltration to fabricate robust, flexible, and transparent, anti-reflective superhydrophobic polymer films on a large scale. Chem Eng J. 2018;350:225-32.
16. Lee S-J, Kim G-M, Kim C-L. Friction and wear reduction effect of glass bubbles embedded in PDMS surface. J Mech Sci Technol. 2022;36(4):1997-2005.
17. Lee S-J, Amanov A, Kim C-L. Tribological properties of microball-embedded polydimethylsiloxane under water-based lubrication conditions. J Mech Sci Technol. 2023;37(8):4281-9.
18. Kim C-L, Jung C-W, Oh Y-J, Kim D-E. A highly flexible transparent conductive electrode based on nanomaterials. NPG Asia Mater. 2017;9(10):e438-438.
19. Yu H, Zhu YB, Jin X, Liu H, Wu HA. Multiscale simulations of shale gas transport in micro/nano-porous shale matrix considering pore structure influence. J Nat Gas Sci Eng. 2019;64:28-40.
20. Zhu H, Dai Z, Tu W. Study on the preparation and performance of low gas permeability trifluoropropyl phenyl silicone rubber. RSC Advances. 2017;7(63):39739-47.
21. Tangjie M, Dongliang Z, Qi Z. Research on the friction characteristics and wear mechanism of a chemical etched surface texture at a high contact pressure during stamping. J Mater Eng Perform. 2024;33(13):6656-74.
22. Mirmohammadi SM, Hoshian S, Jokinen VP, Franssila S. Fabrication of elastic, conductive, wear-resistant superhydrophobic composite material. Sci Rep. 2021;11(1):12646.
23. Lee S-J, Segu DZ, Kim C-L. Effects of chemical etching on surface structure and tribological behavior of silicate substrates. Phys Scr. 2024;99(11):115932.
24. Wang X, Zhang Q. Role of surface roughness in the wettability, surface energy and flotation kinetics of calcite. Powder Technol. 2020;371:55-63.
25. Borjanović V, Bistričić L, Vlasov I, Furić K, Zamboni I, Jakšić M, et al. Influence of proton irradiation on the structure and stability of poly (dimethylsiloxane) and poly (dimethylsiloxane)-nanodiamond composite. J Vac Sci Technol B Microelectron Nanometer Struct Process Meas Phenom. 2009;27(6):2396-403.
26. Atthi N, Sripumkhai W, Pattamang P, Thongsook O, Srihapat A, Meananeatra R, et al. Fabrication of robust PDMS micro-structure with hydrophobic and antifouling properties. Microelectron Eng. 2020;224:111255.
27. Lee S-J, Kim C-L. Multilayered carbon nanotube/adhesive films for human body signal detection sensors. Polym Test. 2024;137:108530.
28. Razafiarison T, Silván U, Meier D, Snedeker JG. Surface-driven collagen self-assembly affects early osteogenic stem cell signaling. Adv Healthc Mater. 2016;5(12):1481-92.
29. Liu TL, Chen Z, Kim C-J. A dynamic Cassie–Baxter model. Soft Matter. 2015;11(8):1589-96.

30. Bormashenko E. Progress in understanding wetting transitions on rough surfaces. Adv Colloid Interface Sci. 2015;222:92-103.
31. Xiao C, Shi P, Yan W, Chen L, Qian L, Kim SH. Thickness and structure of adsorbed water layer and effects on adhesion and friction at nanoasperity contact. Colloids and Interfaces. 2019;3(3):55.
32. Zhang BJ, Park J, Kim KJ, Yoon H. Biologically inspired tunable hydrophilic/hydrophobic surfaces: a copper oxide self-assembly multitier approach. Bioinspir Biomim. 2012;7(3):036011.
33. Gachot C, Rosenkranz A, Hsu SM, Costa HL. A critical assessment of surface texturing for friction and wear improvement. Wear. 2017;372:21-41. .
34. Kaschuk JJ, Al Haj Y, Valdez Garcia J, Kamppinen A, Rojas OJ, Abitbol T, et al. Processing factors affecting roughness, optical and mechanical properties of nanocellulose films for optoelectronics. Carbohydr Polym. 2024;332:121877.
35. Lee S-J, Kim C-L. Effects of the etching process on the surface, friction and wear characteristics of silicone rubber coated with micro-sized ceramic particles. Soft Matter. 2024;20(7):1467-74.
36. Lee S-J, Kim G-M, Kim C-L. Design and evaluation of micro-sized glass bubble embedded PDMS composite for application to haptic forceps. Polym Test. 2023;117:107855. .
37. Liao Z, Huang X, Zhang F, Li Z, Chen S, Shan Q. Effect of WC mass fraction on the microstructure and frictional wear properties of WC/Fe matrix composites. Int J Refract Hard Met. 2023;114:106265. .